Acta Crystallographica Section F
Structural Biology and Crystallization Communications
ISSN 1744-3091

Structures of bacterial biosynthetic arginine decarboxylases

Farhad Forouhar,[a,b] Scott Lew,[a,b] Jayaraman Seetharaman,[a,b] Rong Xiao,[a,c] Thomas B. Acton,[a,c] Gaetano T. Montelione[a,c,d] and Liang Tong[a]*

[a]Northeast Structural Genomics Consortium, USA, [b]Department of Biological Sciences, Columbia University, New York, NY 10027, USA, [c]Center for Advanced Biotechnology and Medicine, Department of Molecular Biology and Biochemistry, Rutgers University, Piscataway, NJ 08854, USA, and [d]Department of Biochemistry, Robert Wood Johnson Medical School, Piscataway, NJ 08854, USA

Correspondence e-mail: ltong@columbia.edu

Received 1 September 2010
Accepted 10 October 2010

PDB References: *C. jejuni* SpeA, 3nzp; *E. coli* SpeA, 3nzq.

Biosynthetic arginine decarboxylase (ADC; also known as SpeA) plays an important role in the biosynthesis of polyamines from arginine in bacteria and plants. SpeA is a pyridoxal-5′-phosphate (PLP)-dependent enzyme and shares weak sequence homology with several other PLP-dependent decarboxylases. Here, the crystal structure of PLP-bound SpeA from *Campylobacter jejuni* is reported at 3.0 Å resolution and that of *Escherichia coli* SpeA in complex with a sulfate ion is reported at 3.1 Å resolution. The structure of the SpeA monomer contains two large domains, an N-terminal TIM-barrel domain followed by a β-sandwich domain, as well as two smaller helical domains. The TIM-barrel and β-sandwich domains share structural homology with several other PLP-dependent decarboxylases, even though the sequence conservation among these enzymes is less than 25%. A similar tetramer is observed for both *C. jejuni* and *E. coli* SpeA, composed of two dimers of tightly associated monomers. The active site of SpeA is located at the interface of this dimer and is formed by residues from the TIM-barrel domain of one monomer and a highly conserved loop in the β-sandwich domain of the other monomer. The PLP cofactor is recognized by hydrogen-bonding, π-stacking and van der Waals interactions.

1. Introduction

Polyamines (putrescine, spermidine and spermine) are involved in a variety of important cellular processes in all living cells, including cell growth and differentiation, DNA replication and repair, RNA synthesis and processing, and protein synthesis and metabolism (Wallace, 2009; Wallace *et al.*, 2003; Tabor & Tabor, 1985). In animals, arginine serves as the primary precursor for the biosynthesis of polyamines through its hydrolysis to ornithine by arginases (Morris, 2004, 2009). Ornithine is then converted to putrescine by ornithine decarboxylase (ODC), which is a proven target for drug action (Wallace, 2009). In bacteria and plants, the biosynthesis of polyamines from arginine proceeds through a different pathway. Arginine is first converted to agmatine by a biosynthetic arginine decarboxylase (ADC; also known as SpeA; Wu & Morris, 1973*a*; Moore & Boyle, 1990), which is then hydrolyzed to generate putrescine and urea by agmatinase (Morris, 2004). These organisms can also produce polyamines through ODC activity.

SpeA is a pyridoxal-5′-phosphate (PLP)-dependent enzyme that is widely distributed in plants and bacteria. It shares weak sequence homology to several other PLP-dependent decarboxylases, especially ODC. Previous biochemical studies suggested that the holoenzyme of *Escherichia coli* SpeA is a tetramer, in which one molecule of PLP is bound to each subunit, with a molecular weight of 70 kDa (Wu & Morris, 1973*a*,*b*). This tetrameric form of the enzyme depends on the presence of an Mg^{2+} ion. In its absence, SpeA exists in an equilibrium between monomeric and dimeric forms, in which the ratio of monomer to dimer population depends on the pH (Wu & Morris, 1973*b*).

E. coli also contains an acid-induced arginine decarboxylase (AdiA) which plays a role in pH homeostasis (Stim & Bennett, 1993).

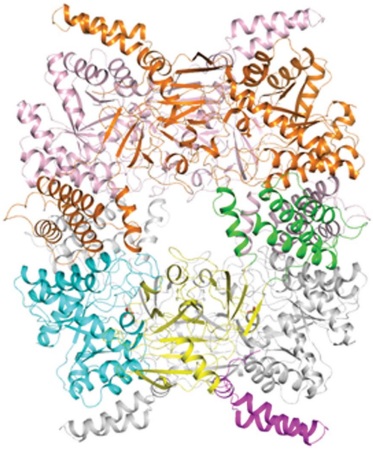

Table 1
Summary of crystallographic information.

Values in parentheses are for the highest resolution shell.

	C. jejuni SpeA (PLP complex)	*E. coli* SpeA (sulfate complex)
Maximum resolution (Å)	3.0	3.1
No. of observations	460394	511680
R_{merge} (%)	9.8 (48.8)	17.2 (76.9)
No. of reflections	93958	41600
Resolution range used in refinement	20–3.0	20–3.1
Completeness (%)	100 (100)	100 (97)
R factor (%)	18.0 (25.5)	20.0 (37.4)
Free *R* factor† (%)	21.9 (29.4)	23.9 (39.2)
R.m.s.d. in bond lengths (Å)	0.009	0.009
R.m.s.d. in bond angles (°)	1.1	1.2
PDB code	3nzp	3nzq

† 5% of the reflections were selected for free *R* calculation.

The two ADCs share only about 10% amino-acid sequence identity and AdiA does not have the same backbone fold as SpeA (Andrell *et al.*, 2009).

Crystallization of *E. coli* (Rodrigez *et al.*, 1994), *Yersinia pestis* (Patel *et al.*, 2004) and *Bacillus subtilis* (Liu *et al.*, 2009) SpeA has been reported, although a crystal structure of SpeA was not available when we initiated this project. In this paper, we describe the crystal structures of the PLP-bound form of SpeA from *Campylobacter jejuni* at 3.0 Å resolution and of *E. coli* SpeA in complex with a sulfate ion at 3.1 Å resolution.

2. Materials and methods

The production of the SpeA proteins from *C. jejuni* and *E. coli* was carried out as part of the high-throughput protein-production process of the Northeast Structural Genomics Consortium (NESG; Acton *et al.*, 2005). These SpeA proteins correspond to NESG targets BR53 and ER600. The full-length *speA* genes from *C. jejuni* (strain NCTC 11168) and *E. coli* (strain K-12) were cloned into a pET21d derivative (Novagen), generating plasmids pBR53-21.11 and pER600-21.16, respectively. The resulting recombinant proteins contain eight non-native residues (LEHHHHHH) at the C-terminus. *E. coli* BL21 (DE3) pMGK cells, a rare-codon-enhanced strain, were transformed with pBR53-21.11 and pER600-21.16. A single isolate was cultured in MJ9 minimal medium (Jansson *et al.*, 1996) supplemented with selenomethionine, lysine, phenylalanine, threonine, isoleucine, leucine and valine for the production of selenomethionine-labeled SpeA (Doublié *et al.*, 1996). Initial growth was carried out at 310 K until the OD_{600} of the culture reached 0.6–0.8. The incubation temperature was then decreased to 290 K and protein expression was induced by the addition of IPTG (isopropyl β-D-1-thiogalactopyranoside) to a final concentration of 1 m*M*. Following overnight incubation, the cells were harvested by centrifugation.

Selenomethionyl SpeA was purified using standard methods. Cell pellets were resuspended in lysis buffer (50 m*M* Tris pH 7.5, 500 m*M* NaCl, 40 m*M* imidazole, 1 m*M* TCEP and 0.02% NaN_3) and disrupted by sonication. The resulting lysate was clarified by centrifugation at 26 000*g* for 45 min at 277 K. The supernatant was loaded onto an ÄKTAxpress system (GE Healthcare) with a two-step protocol consisting of IMAC (HisTrap HP) and gel-filtration (HiLoad 26/60 Superdex 75) chromatography. The purified SpeA proteins were concentrated to 8–10 mg ml^{-1}, flash-frozen in aliquots and used for crystallization screening. The sample purity (>95%) and molecular weight were verified by SDS–PAGE and MALDI–TOF mass spectrometry, respectively. The yields of the purified SpeA proteins from *C. jejuni* and *E. coli* were approximately 22 and 64 mg l^{-1}, respectively. The purified SpeA from *C. jejuni* was yellow in color, whereas that from *E. coli* was colorless, suggesting that the *C. jejuni* SpeA possibly contained the PLP cofactor.

C. jejuni SpeA was crystallized by the microbatch method at 277 K. 2 µl protein solution consisting of *C. jejuni* SpeA (7.9 mg ml^{-1}), 5 m*M* Tris pH 7.5, 100 m*M* NaCl, 5 m*M* DTT and 0.02% NaN_3 was mixed with 2 µl precipitating solution consisting of 100 m*M* bis-tris propane pH 7 and 1.88 *M* sodium sulfate. Yellow hexagonal crystals of SpeA appeared overnight and grew to full size after several days; they were subsequently cryoprotected using 25%(*v*/*v*) glycerol and flash-frozen in liquid propane for data collection at 100 K. The crystallization of *E. coli* SpeA was carried out using a similar method and using a similar protein buffer except that 100 m*M* HEPES pH 8.5 and 1.6 *M* ammonium sulfate were used as precipitants.

The crystals of *C. jejuni* SpeA and *E. coli* SpeA belonged to space group $P3_121$ with unit-cell parameters a = 203.1, c = 101.8 Å and space group $P4_12_12$ with unit-cell parameters a = 192.5, c = 119.9 Å, respectively. There are two monomers of SpeA in the crystallographic asymmetric unit of both enzymes. For *C. jejuni* SpeA, a single-wavelength anomalous diffraction (SAD) data set was collected to 3.0 Å resolution at the peak absorption wavelength of selenium on the X6A beamline of the National Synchrotron Light Source (NSLS). Diffraction images were processed with the *HKL* package (Otwinowski & Minor, 1997) and selenium sites were located with the program *SHELX* (Sheldrick, 2008). *SOLVE*/*RESOLVE* (Terwilliger, 2003) was used for phasing the reflections and for automated model building, which correctly placed 20% of the residues with side chains in each protomer of the asymmetric unit. The majority of the model building was rapidly built manually as the crystal has a large solvent content (72%). Each subunit, including the initiating (seleno)-methionine, was built with the program *XtalView* (McRee, 1999) and refined using *CNS* (Brünger *et al.*, 1998). Noncrystallographic symmetry restraints were applied in most stages of the refinement of the structure. A similar method was used for structure determination of *E. coli* SpeA. The process of model building was facilitated using the refined model of the *C. jejuni* SpeA structure. Data-processing and refinement statistics are summarized in Table 1.

3. Results and discussion

The crystal structures of *C. jejuni* and *E. coli* SpeA were determined using the selenomethionyl single-wavelength anomalous diffraction (SAD) method (Hendrickson, 1991). The crystals generally diffracted X-rays poorly, possibly because of their high solvent content (70%), and the best diffraction data sets were collected after screening many crystals. On the other hand, the quality of the electron-density map after solvent flattening was rather good because of the high solvent content. This is also supported by the low *R* and free *R* values and the excellent agreement with expected geometric parameters for the refined models (Table 1). Residues 190–202 and 422–434 are not included in the *C. jejuni* SpeA structure owing to a lack of electron density. None of the residues of the protein are located in the disallowed region, while 85% of the residues are located in the most favored region of the Ramachandran plot (data not shown). The overall structures of *E. coli* and *C. jejuni* SpeA are similar to each other, with an r.m.s. distance of 1.9 Å among their structurally equivalent C^{α} atoms, consistent with the fact that the two enzymes share 33% amino-acid sequence identity.

The structure of the SpeA monomer contains two large domains, an N-terminal TIM-barrel domain followed by a β-sandwich domain, as well as two smaller helical domains (Figs. 1*a* and 1*b*). The first of these helical domains is an insert into the β-sandwich domain, while the second is formed by residues at the C-terminus.

The asymmetric unit of the crystals contains a tightly associated SpeA dimer, in which the TIM-barrel domain of one subunit is surrounded on three sides by the β-sandwich, insert and C-terminal domains of the other subunit (Fig. 1*c*). A total of 3000 Å^2 of the surface area of each subunit is buried in this dimer interface, indicating that the dimer is likely to be stable, which is supported by our solution light-scattering studies on *E. coli* SpeA (data not shown). The C-terminal, β-sandwich and insert domains provide roughly 1300, 1000 and 700 Å^2 surface-area burial in the dimer interface, respectively.

A tetramer of SpeA can be constructed using crystallographic symmetry in the crystals of both *E. coli* and *C. jejuni* SpeA, with generally similar quaternary organizations (Fig. 1*d*). The insert domain is located in the tetramer interface, burying roughly 1800 Å^2 of its surface area for *E. coli* SpeA. There is a large cavity in the center of both tetramers and the tetramer interface is not tightly packed, presumably owing to the absence of PLP, arginine and magnesium ions. Nonetheless, the fact that a similar tetramer was observed for both enzymes in different crystal forms suggests that this is likely to be the structure of the SpeA holoenzyme tetramer (Wu & Morris, 1973*a*,*b*).

The TIM-barrel and β-sandwich domains of SpeA have many structural homologs among various PLP-dependent decarboxylases based on a search of the Protein Data Bank with the *DaliLite* program (Holm *et al.*, 2008). The closest structural homologs include diaminopimelate decarboxylase (DAPDC; *Z* score of 35.2, an r.m.s.d. of 2.9 Å for 414 aligned residues and 25% sequence identity with SpeA; Ray *et al.*, 2002), lysine/ornithine decarboxylase (L/ODC; *Z* score of 31.6, an r.m.s.d. of 3.1 Å for 356 aligned residues and 19%

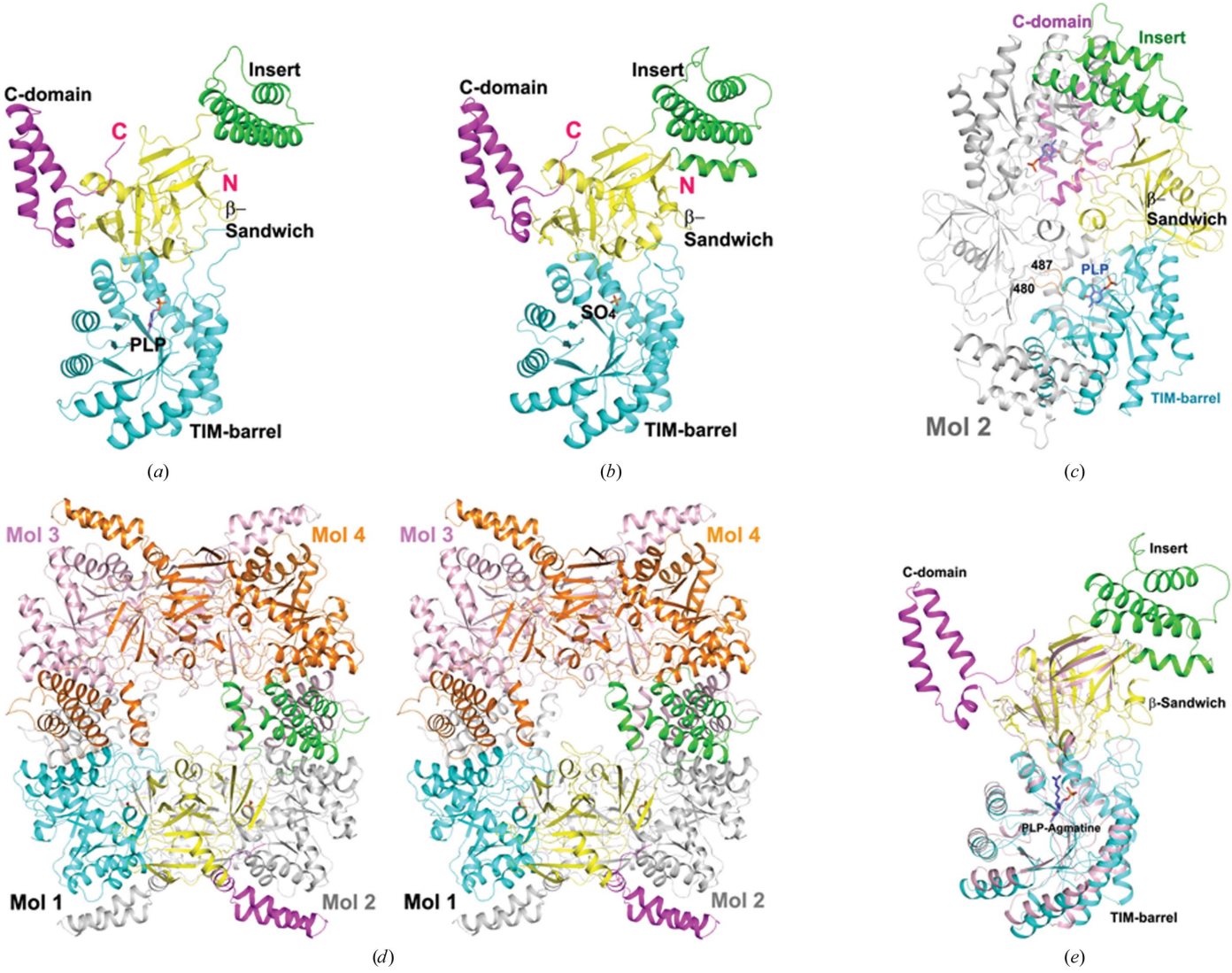

Figure 1
Crystal structures of bacterial biosynthetic arginine decarboxylases (ADC, SpeA). (*a*) Structure of the *C. jejuni* SpeA monomer in complex with PLP. The four domains, TIM-barrel, β-sandwich, insert and C-terminal domain, are colored cyan, yellow, green and magenta, respectively. The PLP cofactor (light blue C atoms) is shown as a ball-and-stick model. (*b*) Structure of the *E. coli* SpeA monomer. A sulfate ion is located in the phosphate-binding site of PLP. (*c*) Structure of the *C. jejuni* SpeA dimer. The second monomer is colored gray, except for the loop that reaches into the active site of the first monomer, which is colored orange and its residue range is indicated. (*d*) Stereo drawing of the structure of the *E. coli* SpeA tetramer. (*e*) Superposition of the structure of the *E. coli* SpeA monomer (colored by domains) and ADC from *P. bursaria* Chlorella virus (pink) in complex with PLP–agmatine (Shah *et al.*, 2007). All structural figures were created with *PyMOL* (http://www.pymol.org).

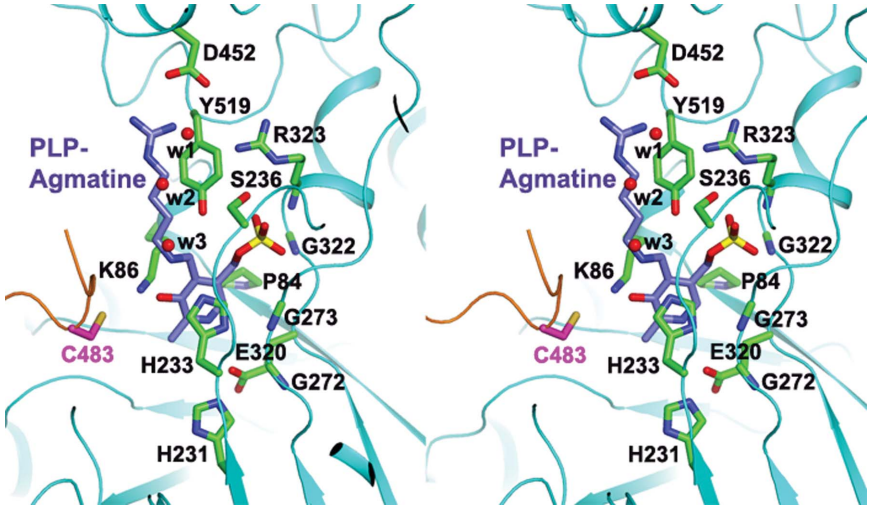

Figure 2
The active site of SpeA. Stereo drawing of the interactions between the PLP cofactor and *C. jejuni* SpeA. A model of PLP–agmatine is shown based on a structural overlay with *P. bursaria* Chlorella virus ADC (Shah *et al.*, 2007). The binding mode of PLP is essentially the same in SpeA and this enzyme. Three water molecules in our structure occupying the expected binding site of the Arg substrate are shown as red spheres.

sequence identity; Lee *et al.*, 2007), ODC (*Z* score of 30.4, an r.m.s.d. of 3.0 Å for 340 aligned residues and 21% sequence identity; Jackson *et al.*, 2004) and the *Paramecium bursaria* Chlorella virus ADC (Fig. 1*e*; *Z* score of 29.7, an r.m.s.d. of 3.1 Å for 351 aligned residues and 18% sequence identity; Shah *et al.*, 2007). The strong structural and functional homology of SpeA to these other enzymes suggests that they have evolved from a common ancestor, despite their low degree of sequence conservation. On the other hand, the insert and the C-terminal domains appear to be unique to SpeA (Fig. 1*e*) and mediate the dimerization and tetramerization of SpeA.

The active site of SpeA is located in the TIM-barrel domain, which is also supported by the observation of a bound PLP cofactor in our structure of the *C. jejuni* enzyme (Fig. 2). In addition, the other monomer of the dimer makes crucial contributions to the active site. Specifically, residues 480–487 in the β-sandwich domain of the other monomer are located in the active site (Fig. 1*c*). This loop contains highly conserved residues among SpeA homologs, especially Cys483, which is equivalent to a Cys residue that has been proposed to be the catalytic residue in close structural homologs of SpeA (Shah *et al.*, 2007; Buschiazzo *et al.*, 2006). Therefore, monomers of SpeA are unlikely to be catalytically active.

The phosphate group of PLP is held in place by five hydrogen bonds to the side chains of the conserved residues Ser236 and Tyr519 (from the β-sandwich domain) and to the backbone amides of the invariant residues Gly274, Gly322 and Arg323 (Fig. 2). The pyridoxal group of PLP forms a π-stacking interaction with the side chain of His233 on one face and is positioned against Pro84 on the other face. The N1 atom of PLP makes a hydrogen bond to the side chain of the strictly conserved Glu320. Most of these residues have equivalents in the close structural homologs of SpeA, suggesting that these enzymes share a common mechanism for recognizing the PLP cofactor. In fact, the bound position of PLP is essentially the same in SpeA and the structure of *P. bursaria* Chlorella virus ADC in complex with PLP–agmatine (compare Figs. 1*a* and 1*e*; Shah *et al.*, 2007). Based on this structure, we can also predict the binding site for the Arg substrate, which is occupied by three water molecules in our structure (Fig. 2). The guanidinium group of Arg may interact with the side chain of Asp452.

While this manuscript was in preparation, the crystal structure of *Vibrio vulnificus* ADC was reported (Deng *et al.*, 2010). The overall structure of this ADC is similar to those of *C. jejuni* and *E. coli* SpeA, including the binding mode of the PLP cofactor and the presence of the two helical domains that help to stabilize the tetramer.

We thank Angela Lauricella and George DeTitta for setting up initial crystallization screenings, Rachel Belote, Colleen Ciccosanti and Seema Sahdev for technical assistance, Randy Abramowitz and John Schwanof for setting up the X4A beamline and Jean Jakoncic for setting up the X6A beamline. This research was supported by the Protein Structure Initiative of the National Institutes of Health grants P50 GM062413 and U54 GM074958.

References

Acton, T. B. *et al.* (2005). *Methods Enzymol.* **394**, 210–243.
Andrell, J., Hicks, M. G., Palmer, T., Carpenter, E. P., Iwata, S. & Maher, M. J. (2009). *Biochemistry*, **48**, 3915–3927.
Brünger, A. T., Adams, P. D., Clore, G. M., DeLano, W. L., Gros, P., Grosse-Kunstleve, R. W., Jiang, J.-S., Kuszewski, J., Nilges, M., Pannu, N. S., Read, R. J., Rice, L. M., Simonson, T. & Warren, G. L. (1998). *Acta Cryst.* D**54**, 905–921.
Buschiazzo, A., Goytia, M., Schaeffer, F., Degrave, W., Shepard, W., Gregoire, C., Chamond, N., Cosson, A., Berneman, A., Coatnoan, N., Alzari, P. M. & Minoprio, P. (2006). *Proc. Natl Acad. Sci. USA*, **103**, 1705–1710.
Deng, X., Lee, J., Michael, A. J., Tomchick, D. R., Goldsmith, E. J. & Phillips, M. A. (2010). *J. Biol. Chem.* **285**, 25708–25719.
Doublié, S., Kapp, U., Aberg, A., Brown, K., Strub, K. & Cusack, S. (1996). *FEBS Lett.* **384**, 219–221.
Hendrickson, W. A. (1991). *Science*, **254**, 51–58.
Holm, L., Kaariainen, S., Rosenstrom, P. & Schenkel, A. (2008). *Bioinformatics*, **24**, 2780–2781.
Jackson, L. K., Baldwin, J., Akella, R., Goldsmith, E. J. & Phillips, M. A. (2004). *Biochemistry*, **43**, 12990–12999.
Jansson, M., Li, Y.-C., Jendeberg, L., Anderson, S., Montelione, G. T. & Nilsson, B. (1996). *J. Biomol. NMR*, **7**, 131–141.
Lee, J., Michael, A. J., Martynowski, D., Goldsmith, E. J. & Phillips, M. A. (2007). *J. Biol. Chem.* **282**, 27115–27125.
Liu, X.-Y., Lei, J., Liu, X., Su, X.-D. & Li, L. (2009). *Acta Cryst.* F**65**, 282–284.
McRee, D. E. (1999). *J. Struct. Biol.* **125**, 156–165.
Moore, R. C. & Boyle, S. M. (1990). *J. Bacteriol.* **172**, 4631–4640.
Morris, S. M. Jr (2004). *Curr. Opin. Clin. Nutr. Metab. Care*, **7**, 45–51.
Morris, S. M. Jr (2009). *Br. J. Pharmacol.* **157**, 922–930.
Otwinowski, Z. & Minor, W. (1997). *Methods Enzymol.* **276**, 307–326.
Patel, C. N., Adcock, R. S., Sell, K. G. & Oliveira, M. A. (2004). *Acta Cryst.* D**60**, 2396–2398.

Ray, S. S., Bonanno, J. B., Rajashankar, K. R., Pinho, M. G., He, G., de Lencastre, H., Tomasz, A. & Burley, S. K. (2002). *Structure*, **10**, 1499–1508.
Rodrigez, B. R., Carroll, D. W., Mitchell, D., Momany, C. & Hackert, M. L. (1994). *Acta Cryst.* D**50**, 175–177.
Shah, R., Akella, R., Goldsmith, E. J. & Phillips, M. A. (2007). *Biochemistry*, **46**, 2831–2841.
Sheldrick, G. M. (2008). *Acta Cryst.* A**64**, 112–122.
Stim, K. P. & Bennett, G. N. (1993). *J. Bacteriol.* **175**, 1221–1234.
Tabor, C. W. & Tabor, H. (1985). *Microbiol. Rev.* **49**, 81–99.
Terwilliger, T. C. (2003). *Methods Enzymol.* **374**, 22–37.
Wallace, H. M. (2009). *Essays Biochem.* **46**, 1–9.
Wallace, H. M., Fraser, A. V. & Hughes, A. (2003). *Biochem. J.* **376**, 1–14.
Wu, W. H. & Morris, D. R. (1973*a*). *J. Biol. Chem.* **248**, 1687–1695.
Wu, W. H. & Morris, D. R. (1973*b*). *J. Biol. Chem.* **248**, 1696–1699.